Springer

Journal of Mechanical Science and Technology 22 (2008) 2509~2515

Journal of Mechanical Science and Technology

www.springerlink.com/content/1738-494x
DOI 10.1007/s12206-008-0910-y

# Experimental investigation of mixing-enhanced swirl flows †

Sam-Goo, Lee

*New & Renewable Energy Material Development Center, Chonbuk National University, Jeonbuk, Korea*

(Manuscript Received April 1, 2008; Revised August 19, 2008; Accepted September 10, 2008)

**Abstract**

The experimental objective was to compare disintegration characteristics from the internal mixing pneumatic nozzles under the different operating conditions in terms of swirl angles. For this investigation, supplied air pressures and nozzle configuration ratios were fixed. This experimental comparison is of fundamental importance to the understanding and modeling of turbulent atomization because the axisymmetric swirling flows involve relatively complex interactions. For the measurement, four internal swirl mixing nozzles with axisymmetric holes at swirl angles of $15^o$, $30^o$, $45^o$, and $60^o$ to the central axis were employed, which is responsible for the enhancement of mixing in pneumatic jets. To illustrate the swirl phenomena quantitatively, the distributions of mean velocities, turbulence intensities, and SMD (Sauter mean diameter, or $D_{32}$) variations with different configuration ratio were comparatively analyzed. It indicated that the atomization characteristics are performed well in the case of $30^o$ of swirl angle, and that turbulence intensities are gradually degenerated with the increase of radial distances, showing a slight increment of SMD at downstream region. In particular, measurements showed that nozzle configuration is one of the significant geometrical parameters affecting the spray trajectories.

*Keywords*: Pneumatic jets; SMD (Sauter Mean Diameter); Turbulence intensity; Penetration; Conservation of momentum; Turbulence suppression; Growth rate

## 1. Introduction

Understanding the physics of disintegrationmechanism in pneumatic atomizers will have a fundamental impact on the ability to characterize the optimum nozzle design. From a practical standpoint, it is essential to have a clear understanding of the prerequisites associated with good atomization. In previous experimental reports concerned with swirl mixing atomizers, turbulent behavior has been observed. Feyedelem and Sarpkaya [1] studied the turbulent flowfield created by a round swirling jet. They reported that swirl led to faster spreading and quicker mixing of the jet, and the similarity of the velocity profiles is achieved at distances as close as 4*d* from the nozzle. But for strong swirl jets, similarity is not reached within 10 diameters downstream. Breaking up the liquid issuing from the pneumatic atomizer into multitudinous small droplets is to increase the liquid surface area and to improve the disintegration. In other words, the atomization in two-phase flows is most effectively achieved by generating a high relative velocity between the liquid jet and the surrounding air resulting from higher momentum by the mutual interactions between working fluids.

Much of what is known about important parameters affecting the mixing process has been obtained from experiments with air to liquid mass flow ratio (ALR) and geometric configuration of the nozzle. Recent progress toward an understanding of the disintegration process has been achieved in experimental approaches of the swirling turbulent velocity, and improved results have been obtained [2]. With the

† This paper was recommended for publication in revised form by Associate Editor Jun Sang Park

*Corresponding author. Tel.: +82 63 581 9570, Fax.: +82 63 581 9575
E-mail address: sglee239@chonbuk.ac.kr

development of laser diagnostics, many experimental investigations on turbulent mixing enhancement have been carried out. Han, et al. [3] investigated the velocity field and turbulence structure in the vortex using an LDV system. In an attempt to understand the disintegration mechanism affecting swirl flows, researchers [4-5] measured mean and fluctuating velocities. They showed that the droplet diameter is progressively reduced as the ALR is increased. Kennedy [6] studied the disintegration mechanism and pointed out that the SMD changed linearly with the surface tension while the influence of the viscosity was minimized. To study the flow patterns at the spray boundary region, Lee et al. [7] made phase Doppler particle analyzer.

(PDPA) measurements of the fluctuating quantities and correlations between volume flux and number density. In the experiment, the author showed that the smaller droplets are inwardly entrained from the spray boundary. An attempt has also been made to investigate the advantage of the internal mixing atomizers. Mullinger [8] showed its merits for the internal atomizers that the atomizing fluid can generally be supplied to the mixing region at a higher pressure than the external mixing type.

The aim here is 1) to shed some light on the turbulent mixing flow and disintegration characteristics, and 2) to determine the geometrical effect issuing from the internal mixing swirl jets.

## 2. Experiment arrangement, procedure, and diagnostics

The nozzle configuration used to establish counterswirling mixing of an axisymmetric jet is schematically shown in Fig. 1. The body of the prototype nozzle for generating a counter-flowing spray was fabricated of brass. The discharge orifice diameter ( $d_o$ ) is 2 mm, swirl chamber diameter ( $D_s$ ) is 9 mm, and the length to diameter ratio of the discharge orifice is 0.65 ($l_o \approx 1.3$ mm). The working fluids were flowed through the tangential ports that results in an angular velocity between two fluids, interacted together in the mixing chamber and injected into the quiescent ambient air at room temperature.

The experimental apparatus is shown schematically in Fig. 2. Continuous and steady flowing water and the pulsation-free air are supplied to the mixing chamber from the pressurized storage tank. Working fluids were properly filtered and regulated. A number

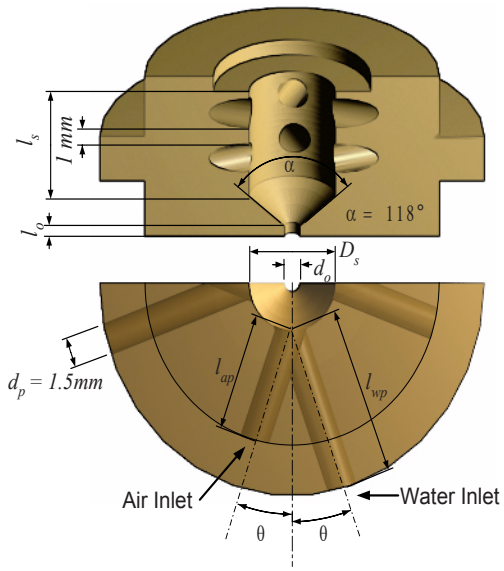


Fig. 1. Specification of nozzle used for the experiment.

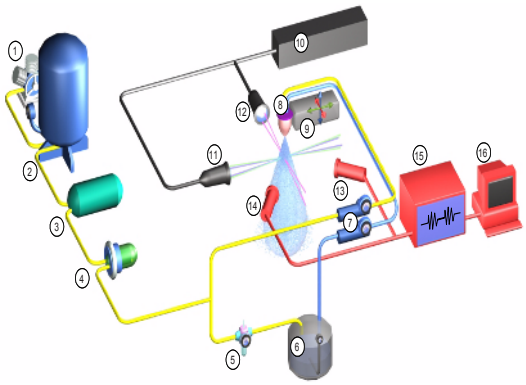


Fig. 2. Experimental setup and diagnostics.

of valves, pressure gauges, and flow meters were set up to control the flow rates. Experiments were conducted for a liquid flow rate kept constant at 7.95 g/s and the air pressures were gradually increased from 20 kPa to 200 kPa, and ALR could be varied from 0.054 to 0.132. A phase Doppler particle anemometer was installed to measure the droplet's spray behavior.

Information is provided here on the individual particle size between 1 μm and 250 μm passing through the measurement volume. The focal lengths of the transmitting and receiving optics were 400 mm and

500 mm, respectively. The photo-multiplier detector voltage of 1400 V was optimized to provide the greatest sensitivity, and 45° scattering was made in the forward direction. Also, a Bragg cell was used to shift the frequency of one beam by 40 MHz to provide directional sensitivity. The data acceptance rate in this experiment was too low for distances less than 20 mm from the nozzle exit. The reasons for the low S/N ratio were usually attributed to the presence of non-spherical particles in the PDPA probe volume. Because the PDPA works on the principle of light scattering by spherical particles, signals of non-spherical particles will be rejected by the instrument. The data acceptance rate varied from 60% to 98% depending on the experimental conditions and the location of the probe volume in relation to the spray geometry. Radial profiles of a geometric sequence space at each measurement locations were obtained at six axial positions downstream from the nozzle exit, respectively. The z coordinate corresponds to the downstream direction at the nozzle exit and y signifies radial outward direction. The measurement volume can be positioned easily at various stations without moving the diagnostic systems in three orthogonal directions by using a computer-controlled traversing system that permits positioning to within 0.02 mm. The droplet quantities were calculated by collecting 10,000 sample data at each point. The sampling time depends on the local number density of drops, and 10 sec. was set as the upper limit to record data. Precautions for accurate measurement were taken to avoid possible sources of error during the experiments, such as mistracking the particles, nozzle vibrations, and the reading of the flow meters, etc. Also, mists of small droplets were discharged to an exhaust system to prevent splashing. To establish the repeatability of the data received, each profile was measured at least twice at different times.

## 3. Results and discussion

Components of mean axial and tangential velocity statistics provide more detailed information of flow field characteristics in swirling jets. The radial profiles of axial and tangential mean velocity distributions both at upstream and downstream regions with four different swirl angles are illustrated in Figs. 3 through 6, respectively. Fig. 3 shows the typical decay rate of mean axial velocity, revealing their axial momentum. Regardless of those different swirl angles,

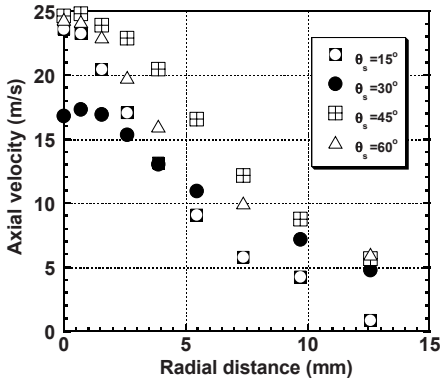


Fig. 3. Variation of axial mean velocity distributions for different swirl angles measured at upstream location of Z/do = 10.

the droplets from both regions are qualitatively considered to be an explicit flow-similarity. Results along the axis at upstream region are particularly helpful in defining the nature of axial momentum despite its swirl component, as shown in Fig. 3. Initially, there is an almost maximum velocity zone that is associated with the potential core region. It indicates the highest momentum ranging from 17-25 m/s at the centerline, but abruptly decreases as a function of radial distance up to 1-7 m/s.

However, the magnitude of tangential velocity components shows quite interesting physical phenomena as indicated in Fig. 4. As the droplets move downstream, the properties in the central region reveal farther downstream propagation due to easy access of atomizing air, whereas the accelerations at the spray boundary (approximately r=10 mm) are discernibly less by the loss of axial momentum and the surrounding drag. As shown in Fig. 4, the minimum value of tangential velocity is along the central axis, which is attributed to the downstream momentum. However, at approximately r=6 mm the tangential velocity increment reaches its highest, revealing a swirl inclination for the turbulent jet to be propagated into the outward. These findings can be attributed to the fact that the spray behavior near the axis seems to have higher momentum and is subsequently subject to higher acceleration even though its geometric conditions are dissimilar.

This spray behavior explains relatively well why the principle of conservation of axial momentum remains constant even though the liquid droplets spread out at an angle due to the centrifugal force. But the effects of nozzle configuration for $\theta_s$=30° are quite

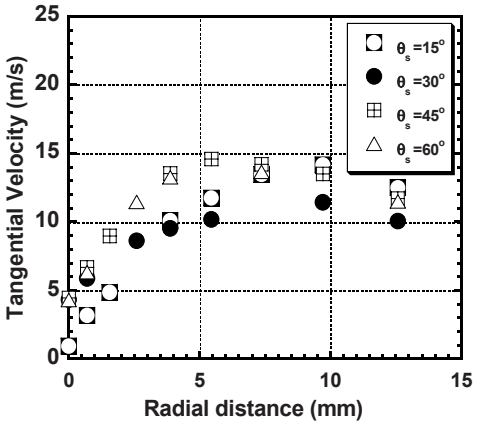


Fig. 4. Variation of tangential mean velocity distributions for different swirl angles measured at upstream location of Z/do = 10.

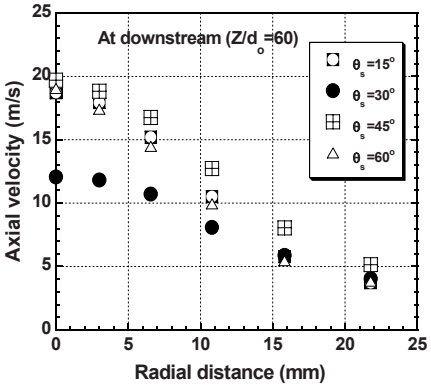


Fig. 5. Variation of mean velocity distributions for different swirl angles measured at downstream location of Z/do=60.

visible, indicating that the distributions for the case of $\theta_s$=30° are much smaller even in the central parts. For the case shown here, the differences both in axial and tangential mean velocity variation can be a possible prognosis to predict and design the optimal swirl atomizer. The effect of swirling flow can be most clearly seen by comparing two profiles, i.e., in axial and tangential components. Even though the spray patterns are similar as shown in Figs. 3 through 6, big differences in magnitudes of velocity as a function of radial distance are apparent between two components. However, the growth rate, or the spray dispersion angle in Figs. 4 and 6 based on the slope of the radial position does not indicate bigger differences among those swirl angles. However, radial distributions for both axial locations as shown in Figs. 3 and 5 are seen to be geometrically symmetric about the spray axis, showing nearly qualitatively consistent value.

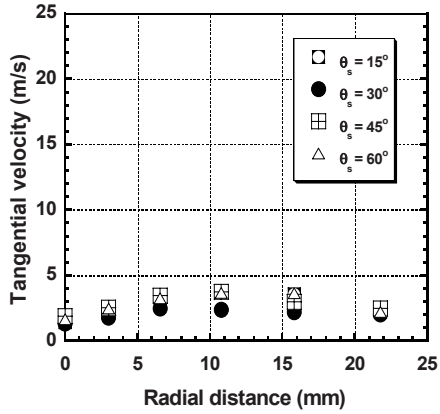


Fig. 6. Variation of mean tangential velocity distributions for different swirl angles measured at downstream location of Z/do=60.

In particular, the tangential distributions at the downstream region are found to be relatively uniform, having a smaller magnitude as shown in Fig. 6. These variations are indeed small when compared to the changes observed in the axial mean velocity distributions. This behavior indicates that the momentum to be spread out tangentially is consistent with the principle of conservation of angular momentum, not the same phenomenon as illustrated in Figs. 3 and 5. Tangential velocities in the center, especially, show minimum values, which comprise the maximum in axial velocity as shown in Figs. 3 and 5. This is mainly because the effects of downward axial penetration and momentum tend to subside the spray dispersion inclination.

On the other hand, the spray trajectory in tangential components at upstream region exhibits a progressive dispersion as it goes to the outer regions up to r=6 mm, shifting the location of maximum velocity at all conditions. After reaching a maximum value, the velocities are sluggishly decreased. But, at the downstream region as shown in Fig. 6, the radial position of maximum tangential value in magnitude is slightly shifted to r=11 mm. Similar but less obvious peaks can be observed. At this location, the axial momentum decreases and, thereby, the swirl inclination increases, supporting the fundamental and typical concepts of swirl atomizer.

The axial turbulence intensities and droplet diameter of SMD variations in Figs. 7 through 10 measured under different swirl angle conditions display the same trends observed in Figs. 3 to 6, indicating quite comparable spray transport.

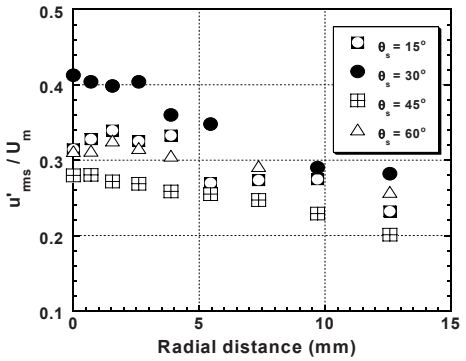


Fig. 7. Distributions of turbulence intensities for different swirl angles measured at upstream location of Z/do=10.

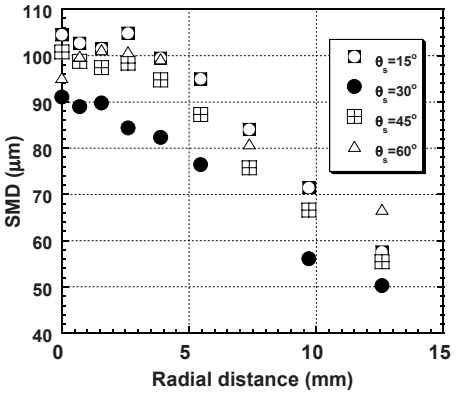


Fig. 8. Distributions of SMD for different swirl angles measured at upstream location of Z/do=10.

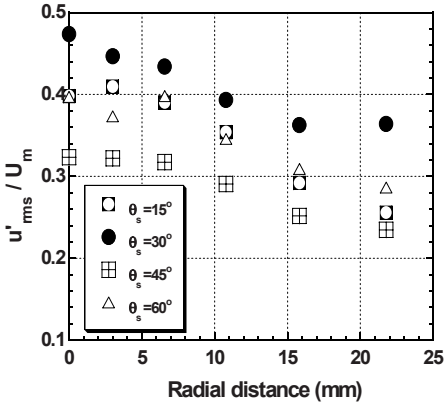


Fig. 9. Distributions of turbulence intensities for different swirl angles measured at downstream location of Z/do=60.

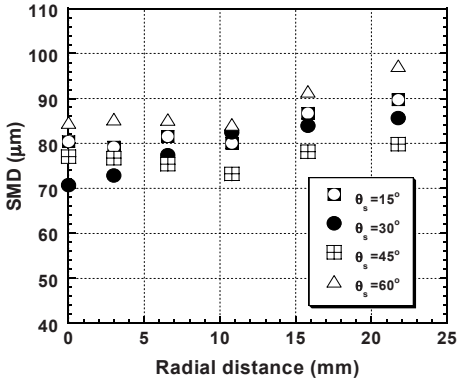


Fig. 10. Distributions of SMD for different swirl angles measured at downstream location of Z/do=60.

The maximum axial turbulence intensities for both cases in Figs. 7 and 9 are located in the center, while having comparatively smaller values toward the spray boundary. Interestingly, for both cases as indicated in Figs. 7 and 9, the magnitude of turbulence intensities for $\theta_s$=30° has the highest value among those four swirl angles. This phenomenon shows a different trend in axial mean velocity variation as discussed in Figs. 3 and 5. Actually, it has nearly the minimum value in mean velocity, causing the droplets with weaker axial momentum to have larger active turbulent disintegration for $\theta_s$=30°.

Comparison of Figs. 7-10 reveals that equivalent peak turbulence levels occur in approximately the center region.

This explains why the spray acquires larger velocity fluctuations for all the cases in the center as an acceleration stage based on the principle of conservation of axial momentum. But, an interesting result can be drawn from this. Even with a higher axial momentum close to the nozzle exit, the downstream turbulence intensities are much higher than the upstream. This is presumably caused by the non-spherical particles or less disintegrated droplets at upstream. Also, the overall turbulence suppression effect is evident at the region despite higher response to the axial momentum. The turbulence data together with the corresponding SMD variations in Figs. 7-10 illustrate that the jet response to swirl angles is noticeably robust and comparatively sensitive to the case of 30° of swirl angle. At higher turbulence intensity levels as shown in Figs. 7 and 9, the lower the SMD diameter on the whole as compared in Figs. 8 and 10.

Consequently, as the sprays are in the process of disintegration, it is considered that better atomization of the droplets could be observed at the downstream region, which is thought to be one of the characteristics in a swirling mixing nozzle. In particular, the

upstream droplets even in the center part are virtually larger than that of the downstream regions. As shown for all the cases, the initial increase in SMD is due to the possibility of coalescence from the less atomized droplets in spite of strong penetration, showing that SMD decreases from approximately 90-105 at upstream to 70-85 at downstream. In contrast to the upstream transport, however, the SMD in the spray periphery gradually increases, which might be explained by the entrainment of small droplets from the outer part to the central region.

This result was reported in the previous research that the smaller droplets in the peripheral region tend to be entrained inwardly and the larger ones are inclined to remain in the region. The smaller droplets at upstream are less abundant in the center region, and the presence of relatively smaller ones near the boundary is ascribed to a distinctive feature in this swirl nozzle. Also, it is interesting to observe that the variation in SMD for $\theta_s$=30$^o$ is the lowest among these nozzles. It is also confirmed that the particles with lower axial momentum cause brisk turbulence fluctuation to bring about better atomization in the spray field.

## 4. Conclusions

Velocity, turbulence intensity and SMD measurements have been obtained in a pneumatic swirl flow. Results were obtained for different swirl angles to study the effects of geometric configuration on the turbulence flow-field characteristics. Pending a more detailed examination of the flow-field development under the increase of ALR as well as the length-to-diameter ratio of nozzle tip, the current findings represent strong characteristics in swirl flow. Although the magnitude of axial velocity distributions for the case of $\theta_s$=30$^o$ is much smaller even in the central parts, it explains the positive effects for disintegration. Tangential velocities in the center, especially, show minimum values, which comprise the maximum in axial velocity. This is mainly because the effects of downward axial penetration and momentum tend to subside the spray dispersion inclination. These findings can be attributed to the fact that the spray behavior near the axis seems to have higher momentum and is subsequently subject to higher acceleration even though its geometric conditions are dissimilar. Especially, the turbulence intensities for the case of $\theta_s$=30$^o$ are higher than the other cases, indicating that strong fluctuations of finer droplets would be developed in this case. The SMD variations illustrate that the jet response to swirl angles is noticeably robust and comparatively sensitive to the case of 30$^o$ of swirl angle. In particular, the upstream droplets even in the center part are virtually larger than that of the downstream regions. There is the possibility that the initial increase in SMD is due to the coalescence from the less atomized droplets in spite of strong penetration. Thus, the nozzle configuration with a swirl angle of 30$^o$ to the central axis is recommended for better disintegration compared to the other ones.

## Nomenclature

$d_o$ : Final discharge orifice diameter
$d_p$ : Diameter of passages for the fluids
$D_s$ : Swirl chamber diameter
$l_o$ : Length of final discharge orifice (1.3 mm)
$l_s$ : Length of swirl chamber (10 mm)
$l_{ap}$ : Length of air passages (10 mm)
$l_{wp}$ : Length of liquid passages (15 mm)
$\theta_s$ : Swirl angle of the inlet passages for the fluids
ALR : Air to liquid mass ratio
$D_{32}$ : Sauter mean diameter
R : Radial distances
$U_m$ : Maximum axial velocity at the centerline
$u'_{rms}$ : Root mean square of the axial fluctuating component
U : Axial mean velocity
W : Tangential mean velocity
Z : Axial distances from the nozzle tip

## References

[1] M. S. Feyedelem and T. Sarpkaya, Free and Near Free Surface Swirling Turbulent Jets, *AIAA Journal*, 36 (3) (1998) 359-364.
[2] A. Mansour and Norman Chigier, Disintegration of liquid sheets, *Phys. Fluids A*., (1990) 706-719.
[3] Y. O. Han, J. G. Leishman and A. J. Coyne, Measurements of the Velocity and Turbulence Structure of a Rotor Tip Vortex, *AIAA Journal*, 35 (3) (1997), 477-485.
[4] S. G. Lee, B. J. Rho, J. Y. Jung and S. J. Kang, Analysis of Turbulent Flow and Disintegration Characteristics Featuring the Counter-Swirl Pneumatic Nozzle, *4th JSME-KSME Thermal Engineering Conference*, Oct. 1-6, Kobe, Japan.
[5] S. G. Lee and B. J. Rho, Atomization characteristics

in pneumatic counterflowing internal mixing nozzle, *KSME International Journal*, 14 (10) (2001), 1131-1142.

[6] J. B. Kennedy, High number SMD Correlations for pressure atomizers, *Journal of Engrg., for Gas Turbines and Power*. (1986) 191-195.

[7] S. G. Lee, B. J. Rho and K. K. Song, Turbulent disintegration characteristics in twin fluid counter flowing atomizer. *39th ALAA Aerospace and Sciences Meeting and Exhibit, AIAA 2001-1047*, (2001), Reno Nevada, USA.

[8] P. J. Mullinger, The design and performance of internal mixing multijet twin fluid atomizers, *Journal of the Institute of Fuel.* (1974) 251-261.